Am J Cancer Res 2026;16(1):70-87
www.ajcr.us /ISSN:2156-6976/ajcr0167901

Original Article

TMEM121 suppresses cervical cancer cell proliferation and migration via interaction with the ERK pathway

Haochen Wang[1*], Siting Xu[1*], Sihui Li[2*], Mei Lin[1], Zhongbei Jiao[1], Jialin Zhao[1], Dan Wu[1], Yanli Huang[1], Siyuan Liu[1], Shanyan Ge[2], Xiushan Wu[1,3], Fang Li[1,4], Lilu Guo[2], Xiongwei Fan[1]

[1]College of Life Sciences, Hunan Normal University, Changsha 410081, Hunan, China; [2]Hunan Provincial Key Laboratory of Regional Hereditary Birth Defects Prevention and Control, Changsha Hospital for Maternal and Child Health Care Affiliated to Hunan Normal University, Changsha 410007, Hunan, China; [3]Guangdong Provincial Key Laboratory of Pathogenesis, Targeted Prevention and Treatment of Heart Disease, Guangzhou 510100, Guangdong, China; [4]Institute of Interdisciplinary Studies, Hunan Normal University, Changsha 410013, Hunan, China. [*]Equal contributors.

Received August 4, 2025; Accepted November 25, 2025; Epub January 15, 2026; Published January 30, 2026

Abstract: TMEM121 is a six-pass transmembrane protein consisting of an N-terminal transmembrane domain (TD; residues 1-284) and a C-terminal polyproline sequence (PP; residues 284-319). In this study, publicly accessible databases were utilized to ascertain that TMEM121 correlates with various cytokines associated with the MAPK signaling pathway in cervical cancer. Furthermore, TMEM121 expression was negatively correlated with ERK expression in cervical cancer tissues. Protein interaction prediction using AlphaFold3 suggested an interaction between TMEM121 and ERK1/2, which was experimentally validated through Co-immunoprecipitation and immunofluorescence analyses. Both full-length TMEM121 and the TD truncator interacted with ERK and downregulate p-ERK1/2 protein levels, thereby inhibiting the proliferation and invasion of cervical cancer cells. In contrast, the PP truncator did not exhibit these effects. RNA-seq analysis further confirmed a significant association between TMEM121 and the MAPK signaling pathway in cervical cancer. Additionally, flow cytometry analysis showed that the ERK inhibitor PD98059 reversed the S phase cell cycle arrest induced by TMEM121 overexpression. Collectively, these findings suggest that TMEM121 exerts its inhibitory effects on the growth, proliferation, and invasion of cervical cancer cells through its interaction with ERK, providing a theoretical basis for the development of novel diagnostic and therapeutic strategies for cervical cancer.

Keywords: TMEM121, MAPK/ERK signaling pathway, RNA-seq, proliferation, cervical cancer

Introduction

Cervical cancer ranks as the fourth most common malignancy among women worldwide, with approximately 604,127 new cases and an estimated 341,831 deaths reported in 2020, with 85% of which occurred in developing countries [1]. Despite the availability of effective screening and vaccination programs, cervical cancer remains a significant challenge in underdeveloped regions [2-5]. The disease primarily comprises squamous cell carcinoma, adenocarcinoma, mixed carcinoma, and small cell carcinoma. Squamous cell carcinoma, arising from squamous epithelial cells on the cervical surface, accounts for 70% to 90% of all cases. HeLa and SiHa cells, commonly used cell lines, serve as representative models for studying cervical adenosquamous carcinoma [6-8]. Cervical cancer originates from the abnormal proliferation of cervical epithelial cells, which progresses to precancerous lesions. As lesions advance, cancer cells penetrate the basement membrane, invade cervical tissues, and develop into invasive carcinoma [9]. The malignancy subsequently spreads to adjacent tissues, lymph nodes, and distant organs [10]. Dysregulated genes involved in DNA replication, mitosis, cell cycle regulation, and metastasis have been implicated in the pathogenesis of squamous cell carcinoma [10, 11]. These alterations drive sustained proliferation, apoptosis

https://doi.org/10.62347/VTCG2993

resistance, and tissue invasion through imbalances in multigene interactions. Key signaling pathways affected include the Mitogen-Activated Protein Kinase (MAPK) and PI3K/Akt/mTOR pathways [12-14].

The MAPK signaling pathway regulates cellular activities, including proliferation, differentiation, survival, and apoptosis [15, 16]. Members of the MAPK family include Extracellular Signal-Regulated Kinase (ERK), p38, and c-Jun N-terminal Kinase (JNK) [17], with the MAPK-ERK pathway playing a central role in cell proliferation and differentiation [16]. The pathway is activated by extracellular signals such as growth factors and cytokines, which bind to receptor tyrosine kinases (RTKs) and trigger phosphorylation cascades. Activated ERK translocates to the nucleus, modulating gene expression by activating transcription factors and regulating physiological processes [18-20]. Identifying inhibitors of the MAPK/ERK pathway offers significant therapeutic potential for cervical cancer [21, 22].

The TMEM121 gene, located on chromosome 14, encodes a six-transmembrane protein consisting of 319 amino acids [23]. Our laboratory was the first to clone TMEM121 and demonstrate its conservation across mammals. Preliminary studies revealed that TMEM121 significantly reduces the migratory capacity of HeLa cells, correlating with a notable down-regulation of B-cell lymphoma 2 (BCL-2), cytosolic protein D1, and cytosolic protein E2, as well as up-regulation of other proteins. TMEM121 has been identified as a novel repressor of cervical carcinogenesis, with promising clinical implications [24]; however, its precise molecular mechanism remains to be elucidated. Previous studies indicate that TMEM121 inhibits MAPK signaling, as evidenced by luciferase reporter assays and suppression of ERK phosphorylation in cardiomyocytes [23]. This suggests that TMEM121 may exert its inhibitory effect on cervical cancer through the ERK pathway.

Structurally, TMEM121 features an N-terminal transmembrane domain with ERK docking site (D domain) and a C-terminal proline-rich sequence (PXXP) [25]. It has been reported that a single nucleotide polymorphism (SNP) in the PXXP sequence binds SH3 domain-containing proteins, potentially regulating ERK pathway activity [26]. Additionally, the D domain may facilitate specific protein-protein interactions, directly or indirectly influencing MAPK pathway activation.

To elucidate the mechanism of TMEM121 in targeting the ERK pathway, we propose integrating bioinformatics and experimental biology approaches. These include analysing gene expression data, protein interaction networks, and signaling pathways, coupled with gene knockdown, overexpression and protein interaction studies. This research aims to provide new insights into the role of TMEM121 as an anti-cancer agent, contributing to novel therapeutic strategies for cervical cancer.

Materials and methods

cBioPortal analysis

cBioPortal for Cancer Genomics (http://cbioportal.org) is a comprehensive, publicly accessible resource for exploring cancer genomics data. The platform currently hosts molecular and clinical data from approximately 5,000 tumor samples across 20 cancer types, enabling researchers to investigate cancer genomics profiles and related attributes. In the present study, cBioPortal was utilized to analyze the differential expression of TMEM121 and key factors of the MAPK pathway in cervical cancer.

The human protein atlas

The Human Protein Atlas (https://www.proteinatlas.org/about) provides a publicly accessible resource comprising 12 discrete sections, including tissue specificity, pathology, structure, and protein interactions. Researchers can freely access transcriptomics and related resources through this platform. In this study, the Human Protein Atlas was employed to investigate the expression of the TMEM121 and ERK proteins in both cervical cancer and adjacent non-cancerous tissues.

The AlphaFold syste

AlphaFold system (https://alphafold.ebi.ac.uk), developed by DeepMind, is an advanced protein structure prediction system that leverages deep learning algorithms to accurately model three-dimensional protein structures based on amino acid sequences. The predic-

tions cover nearly all molecular complexes in the protein database and include confidence scores ranging from 0 to 100, with higher scores indicating greater reliability. This study used AlphaFold to predict the interaction structure between TMEM121 and its truncations with ERK.

The UniProt database

The UniProt database (https://www.uniprot.org/) is a widely-used, comprehensive repository for protein sequence and function annotations, maintained by leading bioinformatics organizations. UniProtKB, the Knowledgebase of UniProt, provides extensive details on protein sequences, lengths, structural domains, subcellular localization, and other functional annotations, assisting researchers in protein functions analysis. In this study, UniProt was used to obtain foundational information on TMEM121.

Simple modular architecture research tool (SMART) website analysis

SMART is a web-based tool designed for identifying and analyzing protein structural domains, particularly in multi-domain proteins. It facilitates the prediction and annotation of functional domains, enabling insights into their biological roles and involvement in specific signaling pathways. This study employed SMART to investigate the structural domain architecture of TMEM121.

Cell culture and transfection

The human cervical cancer cell lines, HeLa and SiHa, were maintained in our laboratory. HeLa and SiHa cells were cultured in DMEM medium supplemented with 10% fetal bovine serum and 1% penicillin-streptomycin-amphotericin B. The cells were incubated at 37°C with 5% CO_2. For overexpression experiments, HeLa and SiHa cells were transfected with the following plasmids: pCMV-Tag2B-TMEM121 (TMEM121), the empty control plasmid pCMV-Tag2B (Control), pSUPER-TMEM121 interfering siRNA (RNAi), its control pSUPER (Control), pCMV-Tag2B-TMEM121-TD (TMEM121-TD), pCMV-Tag2B-TMEM121-PP (TMEM121-PP), and pCMV-HA-ERK1/2 (ERK-HA). Transfection were performed using the Lipo8000 reagent according to the manufacturer's instructions.

Cell counting kit-8 (CCK-8) cell proliferation assay

Following a 24-hours transfection period, cells were harvested, resuspended in medium containing 10% fetal bovine serum, plated in 96-well plates, and incubated for 24, 48, and 72 hours. For cell viability assays, 10 μL of CCK-8 reagent was added to each well, and absorbance was measured at 450 nm after 1 hour of incubation in a 37°C incubator using an enzyme marker (Bio-Rad Laboratories, Inc.).

Transwell invasion assay

To assess cell migration, 24-hours post-transfection, cells were resuspended in serum-free medium and seeded into the upper chamber of a transwell, pre-coated with matrix gel. After 24 hours of incubation at 37°C, cells were fixed with formaldehyde for 30 minutes, stained with crystal violet for 15 minutes, and the upper layer of non-migratory cells was removed using a swab. Migrated cells were observed and photographed under a 10× microscope.

Western blotting

For protein extraction, cells were lysed 48 hours post-transfection in ice-cold RIPA buffer containing protease and phosphatase inhibitors. Protein concentration was determined using the BCA method, and proteins were separated by Sodium Dodecyl Sulfate-Polyacrylamide Gel Electrophoresis (SDS-PAGE) and transferred to methanol-activated PVDF membrane. The membrane was blocked with 6% skim milk at room temperature for 2 hours, followed by overnight incubation with primary antibodies targeting tubulin (MedChemExpress), ERK (Cell Signaling Technology, Inc.), p-ERK (Cell Signaling Technology, Inc.), and TMEM121 (OriGene Technologies, Inc.) at 4°C. After washing the membrane three times with TBST, secondary antibodies were applied at room temperature for 1 hour, followed by three additional washes with TBST. The membrane was developed with an ultra-sensitive ECL chemiluminescent substrate, and densitometry was conducted using ImageJ v1.52a software (http://imagej.org, National Institutes of Health).

Co-immunoprecipitation (Co-IP)

For Co-IP, cells were lysed 48 hours post-transfection in ice-cold RIPA buffer containing protease and phosphatase inhibitors. Pre-treated anti-HA, anti-FLAG and protein A/G immunoprecipitation magnetic beads (Selleck) were incubated with the cell lysate overnight at 4°C. The supernatant was removed following magnetic separation, and the precipitates were washed three times with PBST. The immunocomplexes were then incubated with protein uploading buffer, boiled, and subjected to SDS-PAGE.

Immunofluorescence

For immunofluorescence staining, cells were fixed with formaldehyde for 20 minutes 24 hours post-transfection, washed three times with PBS, and permeabilized with 5% Triton X-100 for 20 minutes. Cells were incubated with 10% foetal bovine serum for 2 hours at room temperature, followed by overnight incubation with primary antibodies against HA and DYKDDDDK tag (Wuhan Proteintech Group Inc.) at 4°C. After three washes with PBST, cells were incubated with fluorescent secondary antibody for 1 hour at room temperature, followed by three washes with PBST. Nuclei were stained with 4', 6-diamidino-2-phenylindole (DAPI) for 5 minutes at room temperature. After final washes, cells were mounted on slides with an anti-fluorescence quencher, sealed with glycerol to prevent light exposure, and observed using a Zeiss Apotome orthotropic fluorescence microscope.

Flow cytometry

Flow cytometry (BD Biosciences) was used to analyze cell cycle and apoptosis. For cell cycle analysis, cells were collected 48 hours after transfection, washed with PBS, and fixed with 70% ethanol at 4°C overnight. Fixed cells were then collected by centrifugation and stained according to the instructions of Propidium Iodide (PI) kit. For apoptosis analysis, cells were washed with PBS and stained according to the instructions of Annexin V-FITC/PI Assay Kit (BD Biosciences).

RNA extraction and reverse transcription quantitative PCR (qRT-PCR)

Cells were collected 48 hours after transfection and total RNA was extracted 48 hours post-transfection using the Vazyme RNA extraction kit (Vazyme Biotech Co., Ltd.) according to the manufacturer's instructions. cDNA synthesis was performed using the Yeasen cDNA synthesis kit (Yeasen Biotechnology, Shanghai, Co., Ltd.). Real-time quantitative PCR was performed using SYBR Premix Ex Taq II (Takara Bio, Inc.), with the following cycling conditions: 50°C for 2 minutes, 95°C for 5 minutes, followed by 40 cycles of 95°C for 15 seconds and 60°C for 40 seconds. GAPDH was used as an internal reference, and the relative expression of genes was calculated using 2^(-ΔΔCq) method.

RNA sequencing

For RNA sequencing, total RNA was extracted from control and TMEM121-overexpressing HeLa cells using QIAzol Lysis Reagent. RNA concentration and purity were examined using a Nanodrop 2000. Following Illumina's guidelines (San Diego, CA), mRNA was enriched, fragmented, and converted to cDNA. After adapter ligation, sequencing was conducted on the NovaSeq X Plus platform (Shanghai Meiji Biomedical Technology Co.). Raw data were quality-controlled using the fastp software, and differential expression was analyzed using DESeq2. Differentially expressed genes were classified based on biological processes, cellular components, and signaling pathways using the Gene Ontology (GO) (http://geneontology.org/) and the Kyoto Encyclopedia of Genes and Genomes (KEGG) (https://www.genome.jp/kegg/) databases.

Statistical analysis

All experiments were performed in triplicate. Statistical analyses were conducted using GraphPad Prism 8.0 (GraphPad Software, Inc., San Diego, CA, USA). Data were first tested for normality via the Shapiro-Wilk test and homogeneity of variance via Levene's test to meet the assumptions of one-way analysis of variance (ANOVA). Differences among multiple groups were analyzed by one-way ANOVA. When a significant overall effect was observed ($P < 0.05$), pairwise comparisons were performed using Tukey's honest significant difference (HSD) test as appropriate. All data are presented as mean ± standard deviation (SD), and statistical significance was set at $p < 0.05$.

Results

TMEM121 is associated with the MAPK signaling pathway involved in cervical cancer regulation

To investigate the role of TMEM121 in cervical cancer regulation, we analyzed the correlation between TMEM121 expression levels and key molecules in the MAPK signaling pathway using the cBioPortal platform. TMEM121 expression levels were found to positively correlate with Insulin-like Growth Factor 2 (IGF2) and IGF1, while showing negative correlation with Jun Proto-Oncogene (JUN), Ste20-Like Kinase (SLK), Specificity Protein 1 (SP1), RAF Proto-Oncogene Serine (RAF1), and ETS Proto-Oncogene 2 (ETS2) (**Figure 1**). No significant correlation was observed between TMEM121 and Epidermal Growth Factor Receptor (EGFR). These results suggest that TMEM121 is closely associated with the expression of MAPK pathway members, potentially contributing to cervical cancer development and progression.

Expression differences of TMEM121 and ERK1/2 in adjacent non-cancerous tissues and cervical cancer tissues

Further analysis using The Human Protein Atlas compared TMEM121 and ERK1/2 expression levels in human cervical cancer tissues and adjacent non-cancerous tissues. Immunohistochemical staining demonstrated significantly decreased TMEM121 expression and increased ERK1/2 expression in cervical cancer tissues compared to adjacent non-cancerous tissues (**Figure 2A**, **2B**), indicating an inverse correlation between the two proteins in pathological tissues (**Figure 2C**).

Interaction between TMEM121 and ERK

Structural predictions using AlphaFold 3 identified potential interaction between TMEM121 and ERK1/2. Specifically, TMEM121's T139 forms a hydrogen bond with ERK1's D338; K213 with ERK1's D179; M1 and V2 with ERK2's D318 and D321, respectively; and R68 with ERK2's D162 (**Figure 3A**, **3B**). These results suggest four potential interaction sites at the molecular level.

To validate these interactions, co-transfection of plasmids expressing TMEM121 and ERK1/2 into HeLa and SiHa cells was followed by immunofluorescence staining, which showed co-localization of TMEM121 and ERK1/2 at the cell membrane (**Figure 3C**). This observation is consistent with the characteristic of TMEM121 as a six-pass transmembrane protein. Co-IP experiments further confirmed this interaction. Immunoprecipitation of HeLa cell lysates with anti-TMEM121 (FLAG) antibodies followed by Western blotting detected ERK1/2-HA in the precipitated complex. Similarly, HA-tagged beads detected TMEM121-FLAG in co-precipitates (**Figure 3D**), confirming a direct or indirect interaction between TMEM121 and ERK1/2.

Interaction between TMEM121 truncated forms and ERK, with the TD truncated form inhibiting ERK activation

Mitogen-activated protein kinase kinase 1 (MEK1) catalyzes ERK phosphorylation through its kinase activity, activating ERK and facilitating downstream signal transduction [17]. TMEM121 is hypothesized to regulate signal transduction processes at the cell membrane. Protein structural information for TMEM121, ERK, and MEK1 was analyzed using the UniProt database, and their domain compositions and interactions are illustrated in **Figure 4A**.

Subsequent experiments explored the distinct biological functions of TMEM121's TD and PP domains. AlphaFold 3 predicted that both domains containing binding sites for ERK1/2. To test this, HeLa cells were transfected with plasmids expressing full-length TMEM121 or its truncated forms (TD and PP truncants). Co-IP experiments demonstrated that both truncants interact with ERK1/2 (**Figure 4B**, **4C**). Western blot analysis revealed that overexpression of full-length TMEM121 or the TD truncator significantly downregulated p-ERK levels, whereas the PP truncator had no effect on p-ERK expression (**Figure 4D**, **4E**). These results suggest that TMEM121 and its TD truncator modulate ERK phosphorylation.

Impact of TMEM121 and its truncated forms on proliferation and invasion of cervical cancer cells

Analysis using the SMART database identified the D domain in MEK1. This domain serves as an essential attachment site for the ERK substrate, promoting its phosphorylation [27]. To

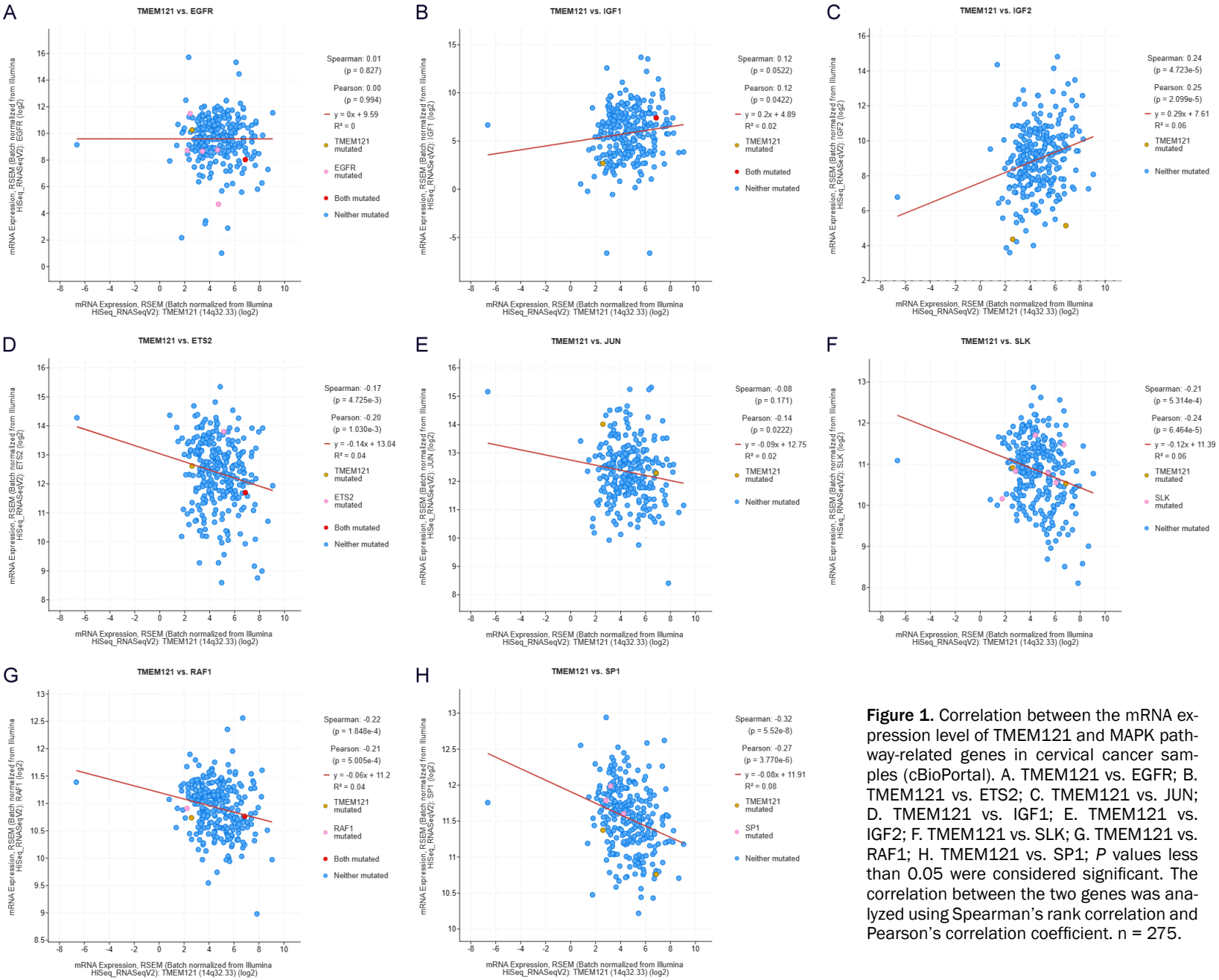

Figure 1. Correlation between the mRNA expression level of TMEM121 and MAPK pathway-related genes in cervical cancer samples (cBioPortal). A. TMEM121 vs. EGFR; B. TMEM121 vs. ETS2; C. TMEM121 vs. JUN; D. TMEM121 vs. IGF1; E. TMEM121 vs. IGF2; F. TMEM121 vs. SLK; G. TMEM121 vs. RAF1; H. TMEM121 vs. SP1; *P* values less than 0.05 were considered significant. The correlation between the two genes was analyzed using Spearman's rank correlation and Pearson's correlation coefficient. n = 275.

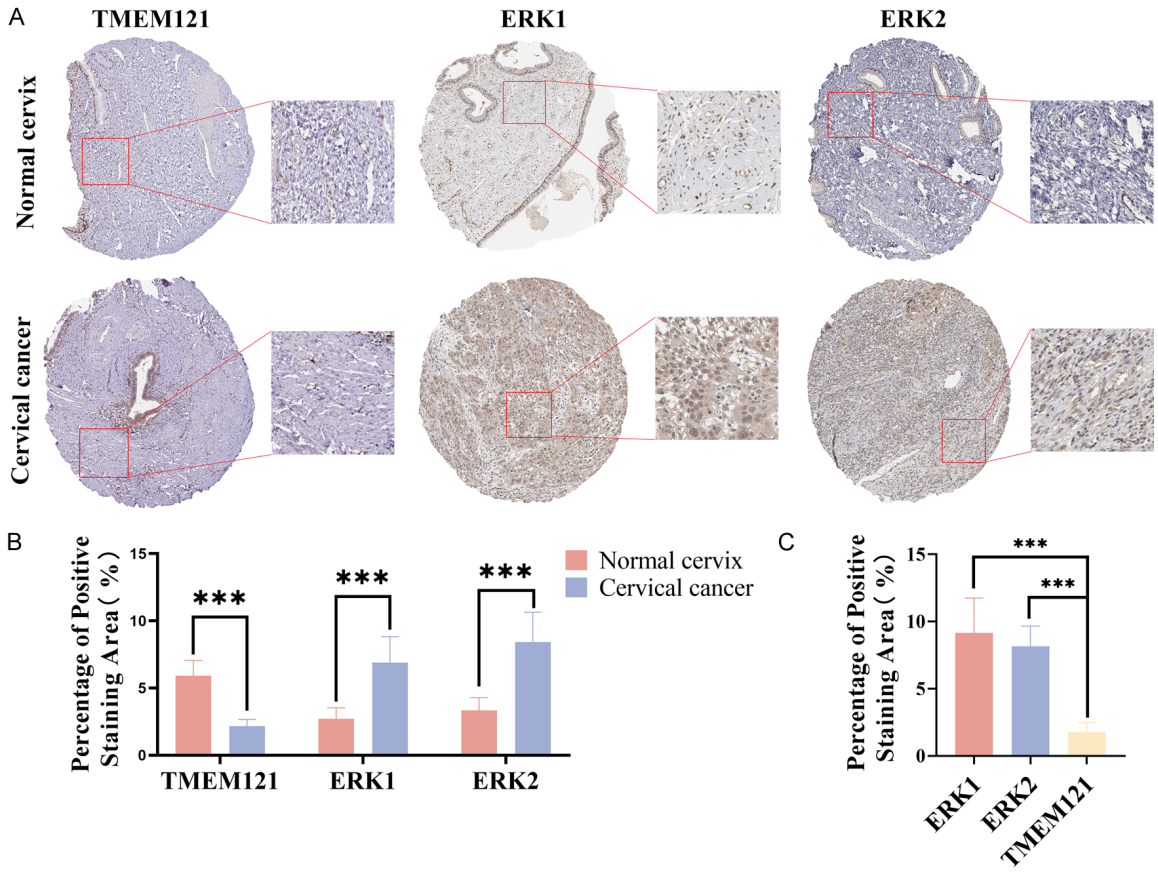

Figure 2. Expression of TMEM121 and ERK1/2 in paracancerous tissues and cervical cancer tissues (The human protein atlas). A, B. Immunohistochemical staining of TMEM121 and ERK1/2 in paracancerous tissues and cervical cancer tissues of patients, and quantitative analysis of the percentage of positively stained area; C. Immunohistochemical staining and quantitative analysis of the percentage of positively stained areas revealed a significant negative correlation between TMEM121 and ERK1/2 expression levels n = 3; ***P < 0.001.

investigate the biological functions of TD truncants containing the D domain in cervical cancer cells, CCK-8 assays were performed (**Figure 5A**). Overexpression of TMEM121 and TD truncants significantly reduced HeLa and SiHa cells viability at 24, 48 and 72 hours, whereas the knockdown of TMEM121 and overexpression of PP truncator showed no significant changes compared to the control group. A transwell invasion assay revealed that overexpression of the TMEM121 and TD truncator significantly reduced HeLa cells invasion, while TMEM121 knockdown increased invasion (**Figure 5E**, **5F**). No discernible changes were observed in the PP group. Flow cytometry analysis showed no significant differences in apoptosis among TMEM121-overexpressing HeLa cells (**Figure 5B**, **5C**). However, immunofluorescence analysis of Ki-67 protein, a tumour cell proliferation marker, demonstrated significantly reduced Ki-67 expression in cells overexpressing TMEM121 and TD truncator, with no changes in the PP group (**Figure 5D**). These results suggest that TMEM121 and TD truncator suppress cervical cancer cells proliferation and invasion by downregulating ERK phosphorylation, independent of apoptosis.

RNA-seq analysis of the impact of TMEM121 overexpression on the multi-gene expression profile in HeLa cells

To further explore TMEM121's role in cervical cancer and its impact on the MAPK signaling pathway, the transcriptome of TMEM121-overexpressing HeLa cells using RNA-seq was analyzed. Total RNA was extracted, and three biological replicates were analyzed per group using the Megji Bio Cloud Platform. Principal Component Analysis (PCA) confirmed the repro-

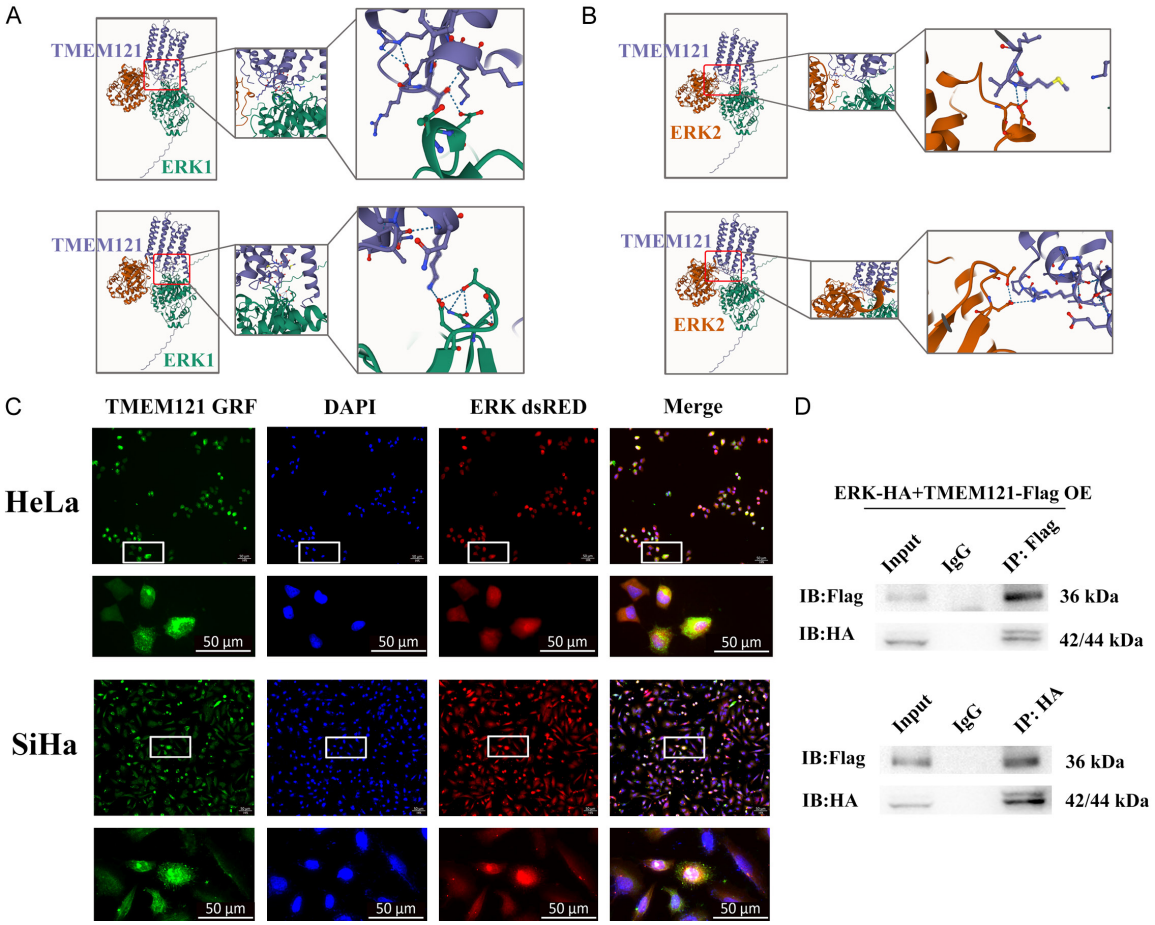

Figure 3. Interaction between TMEM121 and ERK1/2. A. AlphaFold 3-predicted interaction model between TMEM121 and ERK1, showing two interaction sites. TMEM121 is depicted in purple and ERK1 in green. B. AlphaFold 3-predicted interaction model between TMEM121 and ERK2, showing two interaction sites. TMEM121 is depicted in purple and ERK2 in orange. C. Immunofluorescence staining of HeLa and SiHa cells co-transfected with TMEM121 and ERK. ERK is labeled with green fluorescence, TMEM121 with red fluorescence, and the nucleus with blue fluorescence. Scale bar = 50 μm. Magnification is 10× and 40×. D. Confirmation of interaction between TMEM121-FLAG and ERK-HA by Co-IP.

ducibility and reliability of the data (**Figure 6A**). A volcano plot revealed 1,294 differentially expressed genes (DEGs), including 895 upregulated and 399 downregulated DEGs (**Figure 6D**). A clustering heatmap highlighted the top 49 significant DEGs (**Figure 6F**), while a chord diagram identified 20 DEGs related to the cell cycle, migration, proliferation, and MAPK signaling pathway (**Figure 6C**). KEGG pathway and GO enrichment analyses of the DEGs revealed significant involvement of the MAPK signaling pathway (**Figure 6B**) and cellular functions such as DNA replication, cell cycle regulation, and migration. **Figure 6E** displayed the top 20 significant GO terms.

Several key DEGs were selected for qRT-PCR validation, including MAPK pathway-associated genes (Kit ligand (KITLG), delta subunit 1 (CACNA2D1), Conserved helix-loop-helix ubiquitous kinase (CHUK), Mitogen-activated protein kinase 3 (MAPK3), Mitogen-activated protein kinase kinase 7 (MAP2K7) [28-32], cell cycle regulators (Retinoblastoma 1 (RB1), Leukemia inhibitory factor receptor (LIFR), Rho family GTPase 3 (RND3), Rho GTPase-activating protein 5 (ARHGAP5) [33-36], migration-related genes (Mucin 1 (MUC1) and Mesenchymal-epithelial transition factor (MET), an oxidative-reduction gene (Glucose-6-phosphate dehydrogenase (G6PD) [37-41], and a DNA damage

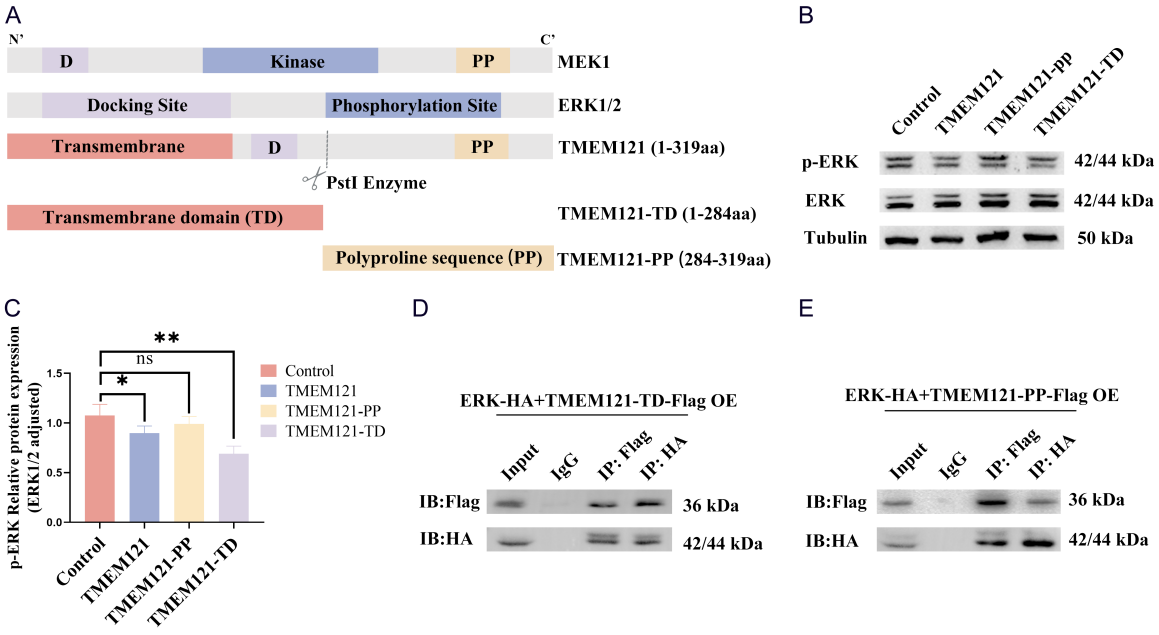

Figure 4. Interaction of TMEM121 truncated forms with ERK and their effect on ERK activation. A. Structural analysis and schematic representation of proteins using the UniProt database. MEK1 includes the D domain (purple), kinase domain (blue), and PP domain (orange); ERK1/2 contains docking sites (purple) and phosphorylation sites (blue); TMEM121 features transmembrane domains (pink), the D domain (purple), and a polyproline sequence (PP domain) (orange). B, C. Western blot of p-ERK expression with grayscale analysis; Control, empty vector; *P < 0.05; **P < 0.01; ns, not significant. D. Confirmation of interaction between TMEM121-TD-FLAG and ERK-HA by Co-IP. E. Confirmation of interaction between TMEM121-PP-FLAG and ERK-HA.

repair gene (Alpha-thalassemia (ATRX)) [42]. The qRT-PCR results (**Figure 7**) confirmed that the expression changes of these 13 DEGs were consistent with the RNA-seq data.

TMEM121 inhibits cervical cancer cell proliferation and invasion by suppressing ERK phosphorylation

PD98059, a specific inhibitor of ERK phosphorylation, blocks MEK1 activation upstream of ERK. To investigate whether TMEM121 can suppress the oncological function of HeLa cells lacking ERK phosphorylation, flow cytometry and transwell invasion assays were performed. As shown in **Figure 8A**, TMEM121 overexpression increased the proportion of HeLa cells in the S-phase cells while reducing those in the G1/G0 phase, indicating S-phase arrest. This effect was abolished upon treatment with PD98059. Western blot analysis showed that ERK phosphorylation levels were significantly reduced following overexpression of TMEM121 in both HeLa and SiHa cells (**Figure 8B**, **8D-F**). PD98059 treatment prominently suppressed p-ERK expression regardless of TMEM121 overexpression. However, there were no significant differences in the levels of ERK phosphorylation between control and TMEM121-overexpressed groups in PD98059-treated cells. Transwell invasion assay further demonstrated that PD98059 treatment reversed the reduction in HeLa cell invasion caused by TMEM121 overexpression (**Figure 8C**). The results confirm that TMEM121 regulates cervical cancer cells proliferation and invasion by regulating p-ERK expression through its interaction with ERK.

Discussion

In this study, we employed bioinformatics and experimental biology to demonstrate that TMEM121 inhibits the proliferation and migration of HeLa and SiHa cells. The key findings are as follows: (1) bioinformatics analysis revealed a negative correlation between TMEM121 and ERK expression in cervical cancer tissues; (2) structural analysis demonstrated that both domains of TMEM121 interact with ERK, with the TD truncator exerting an inhibitory effect on cervical cancer; and (3) inhi-

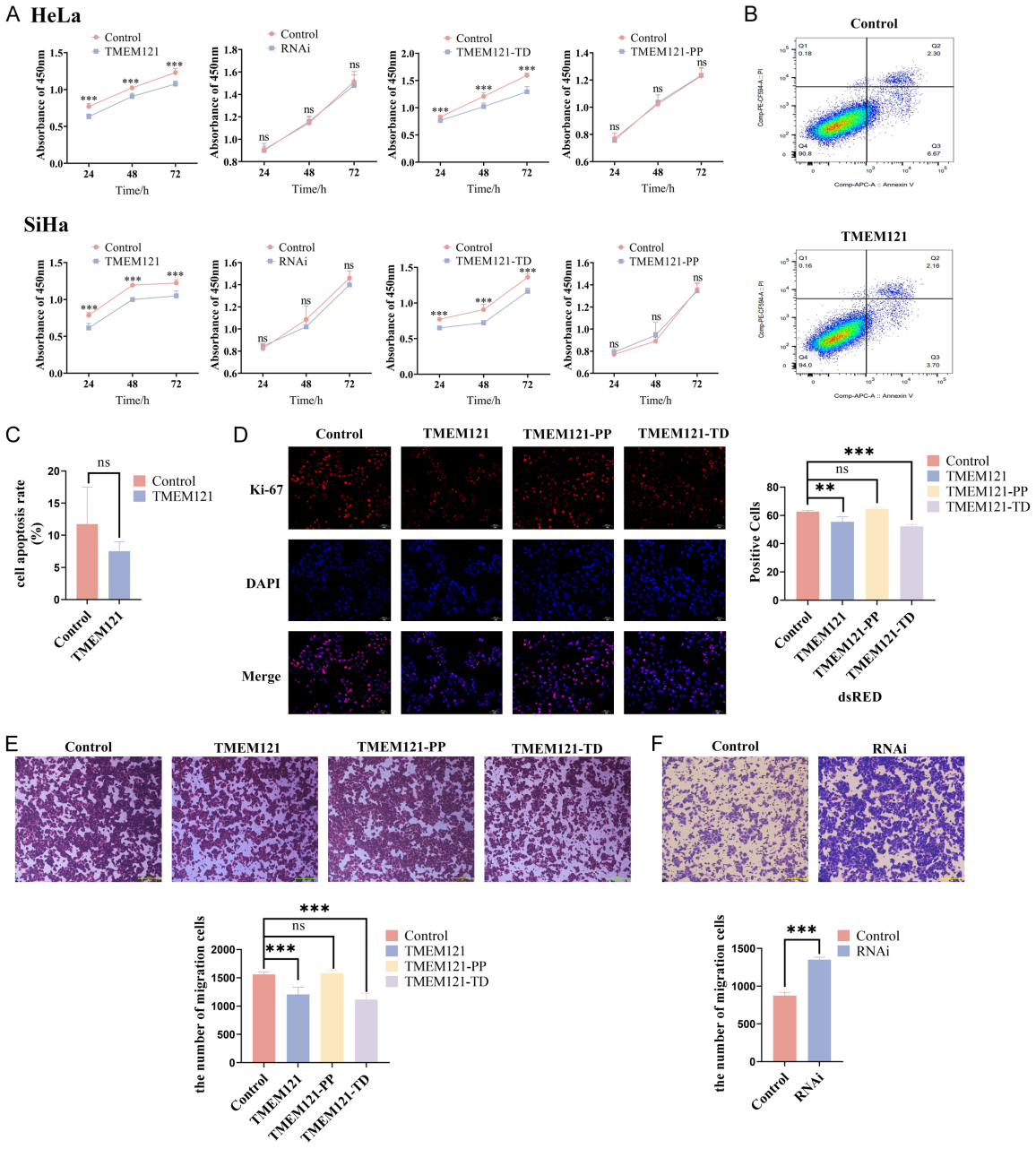

Figure 5. TMEM121 and truncants influence proliferation and invasion of cervical cancer cells. A. CCK-8 cell viability assay in HeLa and SiHa cells; B, C. Effect of TMEM121 on cell apoptosis by flow cytometry and quantitative analysis of counted apoptotic cells; D. Immunofluorescence of Ki-67 expression in HeLa cells and quantitative analysis of fluorescence intensity, red fluorescence labelling of Ki-67, blue fluorescence labelling of cell nucleus, scale bar = 200 μm. Magnification is 10×; E, F. Effect of TMEM121 and truncants on cell invasion by transwell assay and quantitative analysis, scale bar = 200 μm. Magnification is 10×. Control: empty vector; RNAi: RNA interference; TMEM121: overexpression, **P < 0.01; ***P < 0.001; ns, not significantly different.

bition of ERK phosphorylation negated the inhibitory effect of TMEM121. These results suggest that TMEM121 modulates cervical cancer progression through interactions with ERK, highlighting its potential as a therapeutic target.

Using UALCAN, we analyzed TMEM121 expression levels across cervical cancer samples from the TCGA database. TMEM121 expression was significantly reduced in cancer subgroups compared to normal tissues. Consistent with our results, the methylation level of TMEM121

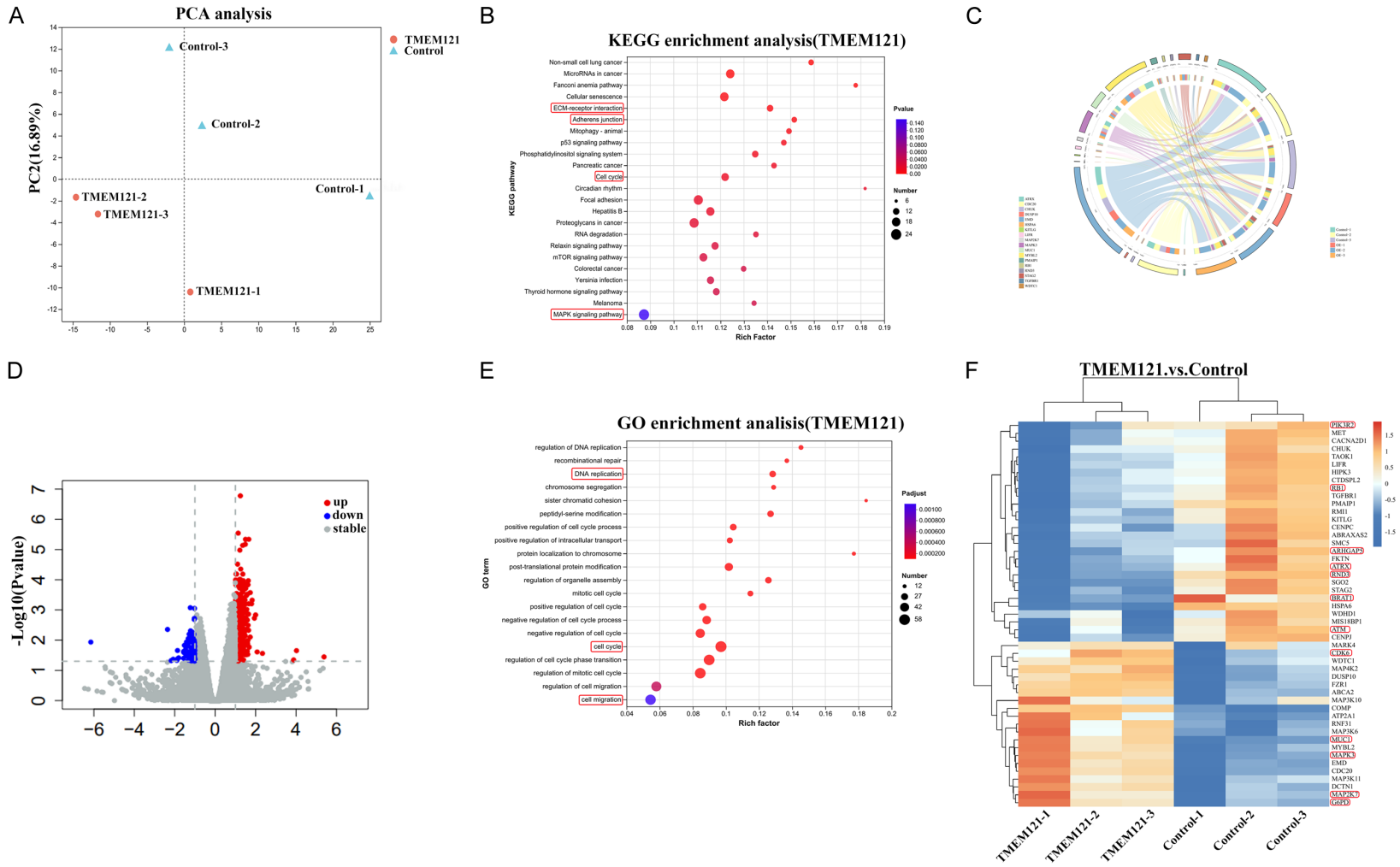

Figure 6. Expression and characterisation of TMEM121 in cervical cancer. A. PCA analysis of triplicates. B. 23 identified significantly activated signaling pathways based on KEGG analysis. C. Chordal plots of top 20 DEGs associated with TMEM121. D. Volcano plots of DEGs. E. Top 20 significantly activated biological processes based on GO analysis. F. Clustering heatmap of DEGs associated with TMEM121. Control: empty vector; TMEM121 overexpression was identified through the application of a log2FC threshold of ≥ 0.80 and a *p*-value of ≤ 0.05.

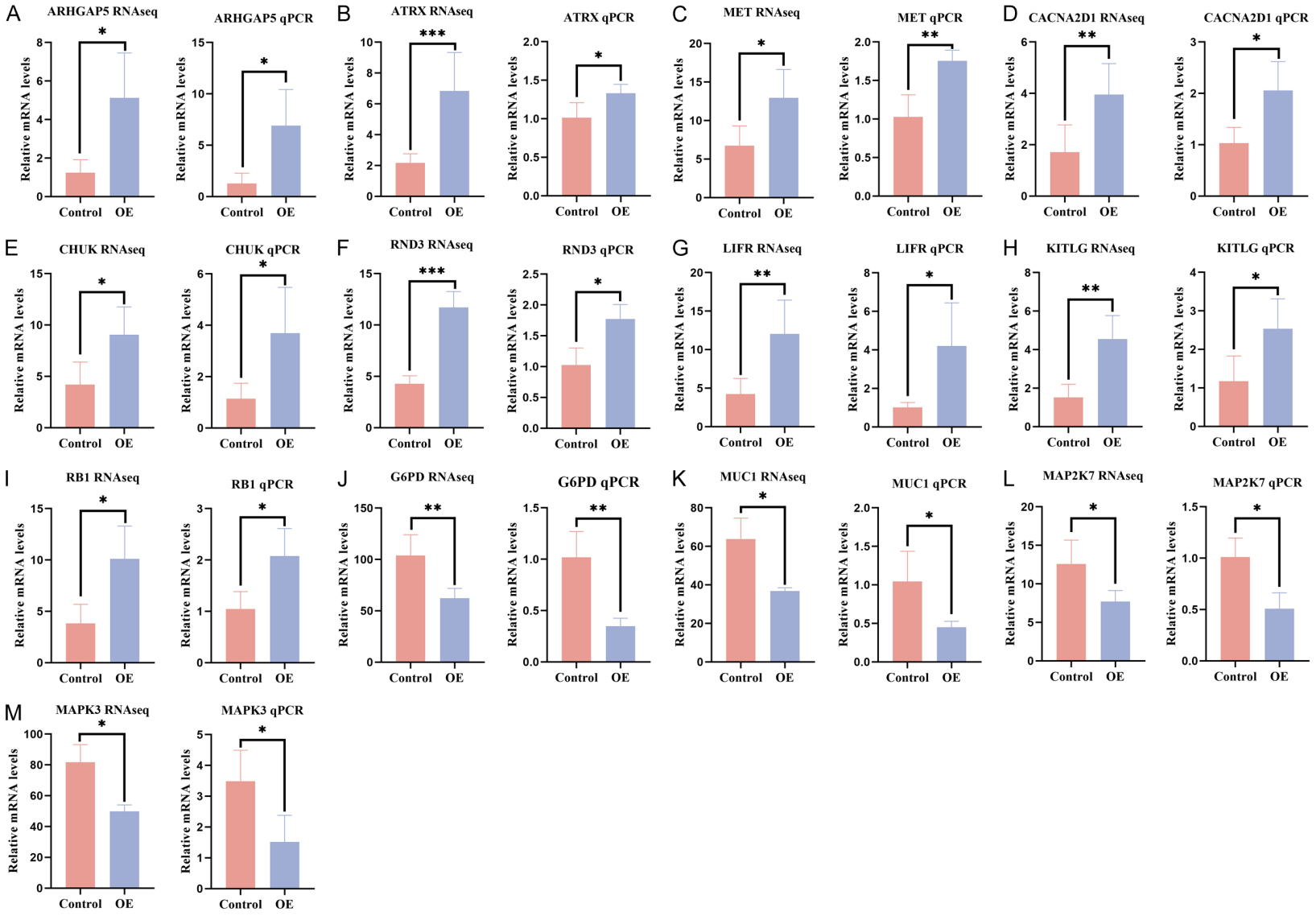

Figure 7. Differentially expressed genes detection by RNA-seq following TMEM121 overexpression and validation by qRT-PCR. Control: empty vector; TMEM121: overexpression. *P < 0.05, **P < 0.01, ***P < 0.001.

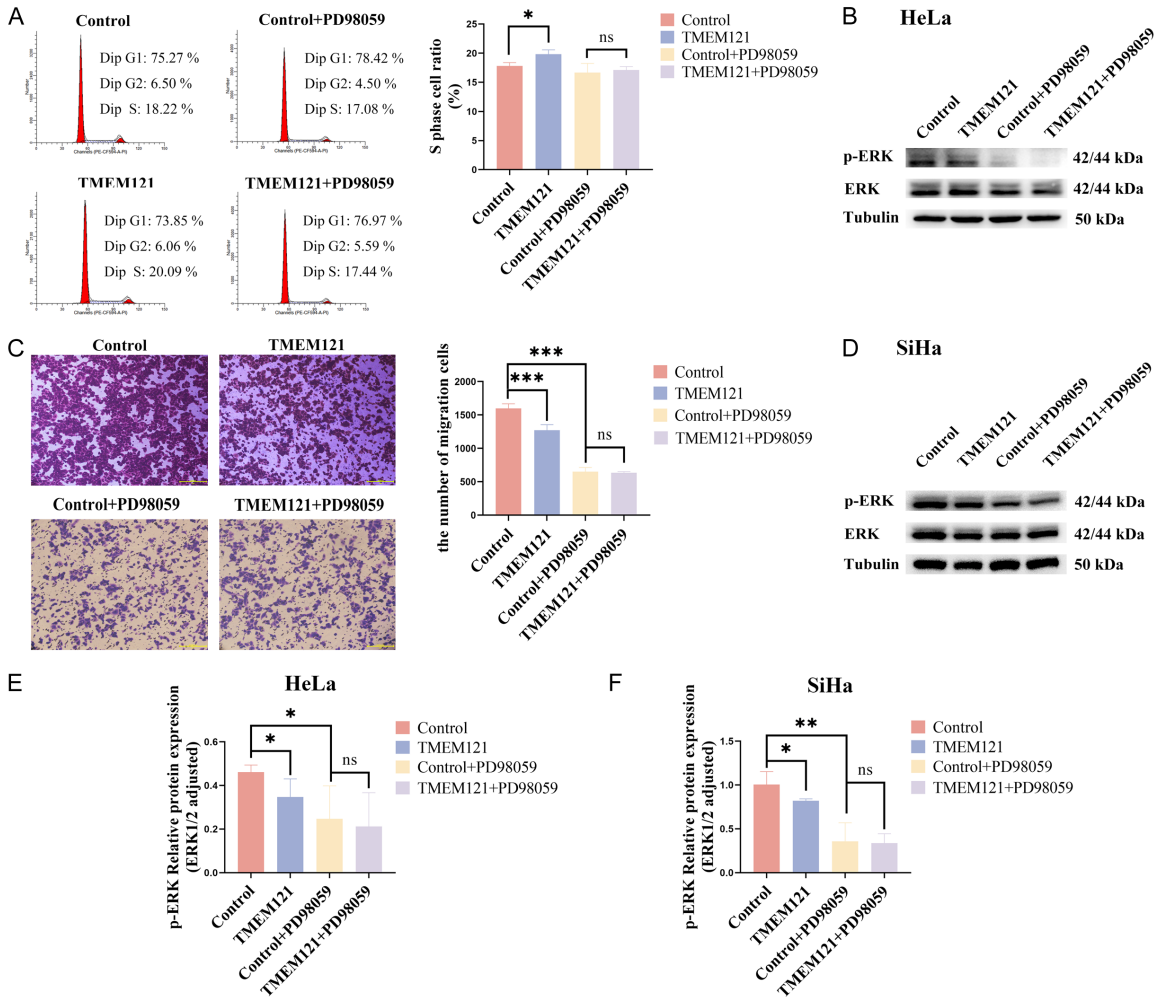

Figure 8. Inhibition of TMEM121 on cell proliferation and invasion through suppressing ERK phosphorylation. A. Effect of TMEM121 on cell cycle by flow cytometry and quantitative analysis of the proportion of S-phase cells. C. Cell migratory ability detection by transwell invasion assay; scale bar = 200 μm. Magnification is 10×. B, D-F. Western blot of p-ERK expression with grey scale analysis; Control: empty vector; TMEM121: overexpression; *P < 0. 05; **P < 0.01; ***P < 0.001; ns, not significantly different.

promoter was significantly increased in various cancerous tissues in comparison to normal tissues [24]. Subsequent analyses confirmed diminished TMEM121 expression and elevated ERK1/2 expression in cervical cancer tissues. Human Protein Atlas revealed a negative correlation between TMEM121 and ERK1/2 expression, suggesting that low TMEM121 levels may promote tumor progression by activating the ERK1/2 signaling pathway.

AlphaFold 3 predicted four interaction sites between TMEM121 and ERK1/2, which were confirmed using Co-IP. Both the full-length and truncated form of TMEM121 were investigated. The addition of TD truncator inhibited cervical cancer cell proliferation and invasion, accompanied by reduced p-ERK levels. Notably, PD98059 (an ERK inhibitor that also targets p-ERK activity) did not further enhance this inhibitory effect when co-administered; instead, the suppressive phenotype mediated by the TD truncator remained consistent. This observation supports that TMEM121 inhibits p-ERK through direct interaction with ERK1/2, thereby impairing cervical cancer cell function - consistent with the shared target of TMEM121 and PD98059 in the ERK signaling pathway. The low expression of TMEM121, coupled with high ERK1/2 expression, further supports the hypothesis that TMEM121 loss deregulates ERK signaling, contributing to cervical cancer

progression. RNA-seq analysis demonstrated that TMEM121 upregulates ARHGAP5 and RND3, downstream targets of ERK signaling [43, 44]. ARHGAP5 encodes a RhoA GTPase-activating protein, which regulates cell migration by inactivating RhoA [45, 46]. RND3, a member of Rho GTPases family, influences cell motility, cytoskeletal reorganization, and intercellular adhesion [47, 48]. The inhibitory effects of TMEM121 on cervical cancer cell migration may extend beyond the ERK pathway. A recent study demonstrated that sustained inhibition of ERK can prevent the transition of cancer cells from the G1 to the S phase, resulting in a G1 phase blockade and consequently slowing cell proliferation [49]. Interestingly, TMEM121 was also shown to induce S phase cell cycle block, as evidenced by CCK-8 assays and cell cycle analyses, which was in line with our previous study [24]. This effect was not associated with increased apoptosis, as flow cytometry demonstrated no significant changes in cell apoptosis. Instead, the reduction in cell numbers was attributed to inhibited proliferation, corroborated by reduced Ki-67 expression. Our RNA-seq data suggest the involvement of an unidentified factor distinct from ERK signaling in mediating the S phase block, providing new insights into the multifaceted role of TMEM121 in regulating cervical cancer progression.

The RNA-seq results (**Figure 6F**) demonstrated that Cyclin-Dependent Kinase 6 (CDK6) expression was significantly elevated, indicating its ability to bind cyclin D, form an active complex, and drive the G1-to-S phase transition. This observation aligns with our previous studies [50-53]. Furthermore, BRCA1-Associated ATM Activator 1 (BRAT1) expression was found to be down-regulated. BRAT1 is known to activate the G2/M checkpoint by interacting with DNA repair factors, such as Breast Cancer 1 (BRCA1) and Ataxia telangiectasia mutated (ATM), thereby allowing cells to halt the cell cycle in response to DNA damage [54]. Concurrently, the expression of ATRX, which promotes DNA damage detection, is diminished, thereby preventing cells from entering mitosis before repair [42]. These findings suggest that TMEM121 overexpression facilitates the G1-to-S phase transition, resulting in S phase arrest, while inhibiting the S-to-G2/M phase progression.

It is noteworthy that the expression of Phosphoinositide-3-kinase regulatory subunit 2 (PIK3R2), a molecule linked to the PI3K-AKT signaling pathway, was significantly reduced, indicating that TMEM121 may impede cervical cancer cell proliferation via this pathway. We previously reported that reduced p-AKT expression effectively prevents cancer cell migration. Bioinformatics analysis further revealed that TMEM121 expression is positively correlated with AKT Serine/Threonine Kinase 1 (AKT1) and negatively correlated with Phosphatidylinositol-4,5-bisphosphate3-kinase catalytic subunit beta (PIK3CB), Caspase 3 (CASP3), and Cadherin 1 (CDH1), key molecules in the PI3K/AKT signaling pathway [24]. Therefore, we hypothesize that AKT1 regulates cell cycle progression by enhancing Cyclin D expression and activating CDK4/6, driving cells into S phase. Additionally, AKT1 activates downstream targets that support cell growth and proliferation, further propelling the S phase transition [55-58]. Although these findings provide valuable insights, further studies are required to confirm the precise mechanism by which TMEM121 regulates cell proliferation.

Intriguingly, PP truncator does not exhibit the same inhibitory effect on cervical cancer cell proliferation and invasion as the TD truncator. This suggests that TMEM121 primarily relies on the TD truncator for its anti-cancer function. The TD truncator contains the D-domain, a conserved structural motif that interacts with ERK. TMEM121 lacks a kinase domain like that of MEK1, while cellular sub-localisation experiments demonstrated that TMEM121 co-localised with ERK on the membrane. Based on these findings, we hypothesize that TMEM121 inhibits ERK phosphorylation by competing with MEK1 through its D-domain, thereby sequestering ERK on the membrane and blocking its binding to MEK1. This membrane localization also confines the nuclear translocation of p-ERK. In contrast, the PP truncator enhances the binding of TMEM121 to ERK and promotes ERK membrane localization, yet lacks inherent inhibitory activity toward ERK (**Figure 9**). The D domain facilitates protein-protein interaction with the D recruitment site of ERK1 and ERK2, which are essential for RAS-dependent cell transformation and cancer cell survival [59]. Thus, targeting this interaction may be an effective strategy for cancer therapy. If TMEM121 exerts its effects via the D domain, artificial modifications of TD could enable the development of small molecule peptide drugs that specifically inhibit ERK signaling in cervical

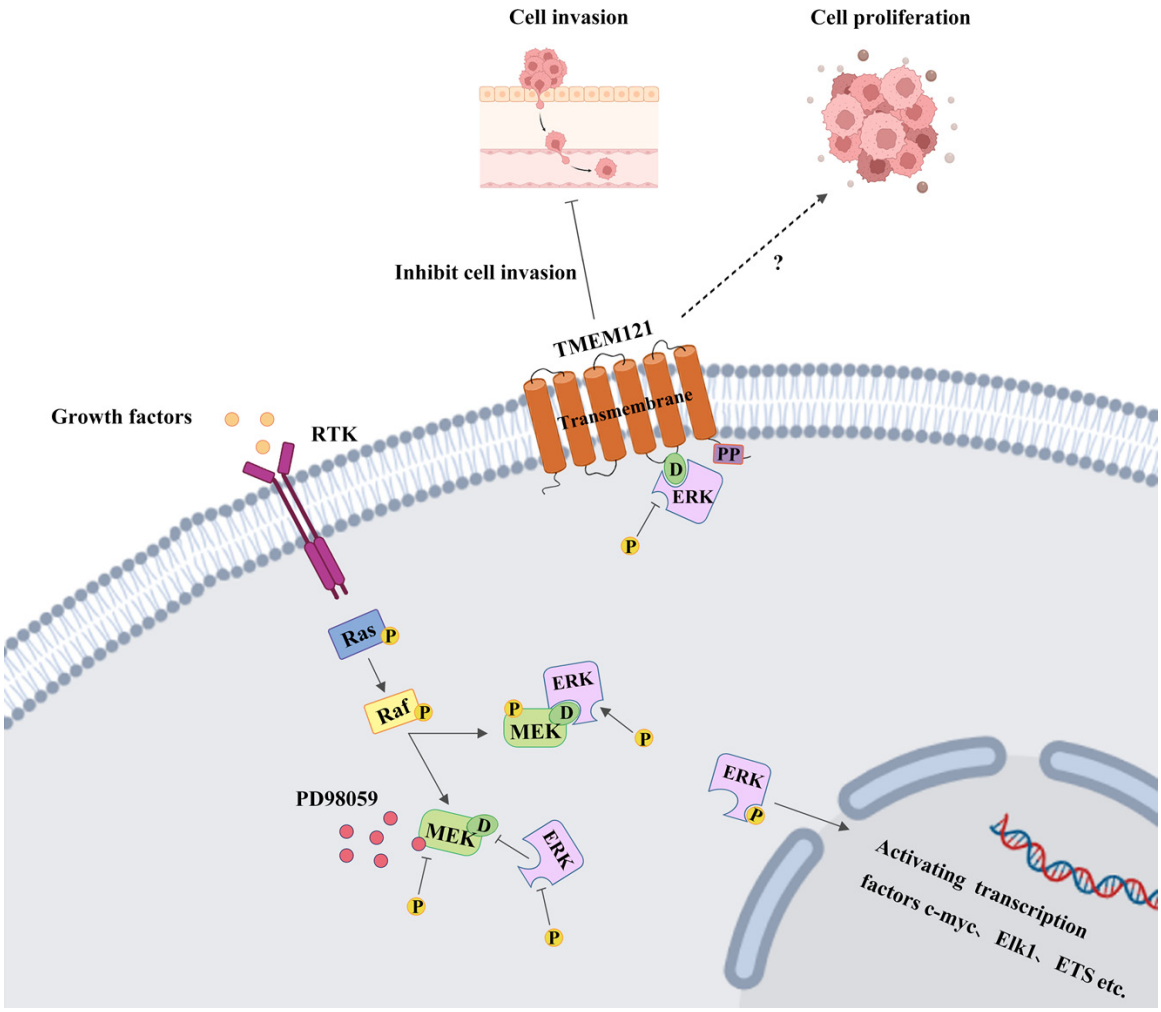

Figure 9. The potential mechanism of action of TMEM121.

cancer. Small molecule peptides offer significant advantages, including high specificity, efficient cellular penetration, and minimal adverse effects.

In conclusion, this study elucidates the pivotal role of TMEM121 in suppressing cervical cancer cell proliferation and migration. For the first time, we used in vitro experiments to explore the mechanism of action of TMEM121 in suppressing cervical cancer progression through ERK reciprocal inhibition. These findings provide a novel perspective on personalised medicine, targeted therapy, and precision diagnostics for cervical cancer.

Acknowledgements

This work was supported by the National Natural Science Foundation of China (Grant Nos. 81970324, 81800289); the Special Project of the National Natural Science Foundation of China (Grant No. 42542044); the Open Research Fund of Hunan Provincial Key Laboratory of Regional Hereditary Birth Defects Prevention and Control (Grant No. HPKL2024002); and the Scientific Research Foundation of Hunan Provincial Educational Committee of China (Grant Nos. 23A0082, 202401000473, Z2024167).

Disclosure of conflict of interest

All authors declare no competing financial or non-financial interests in relation to the work described in this manuscript.

Abbreviations

MAPK, Mitogen-Activated Protein Kinase; ERK, Extracellular Signal-Regulated Kinase; JNK,

c-Jun N-terminal Kinase; RTKs, receptor tyrosine kinases; BCL-2, B-cell lymphoma 2; SNP, single nucleotide polymorphism; SMART, Simple Modular Architecture Research Tool; CCK-8, Cell Counting Kit-8; SDS-PAGE, Sodium Dodecyl Sulfate-Polyacrylamide Gel Electrophoresis; Co-IP, Co-Immunoprecipitation; DAPI, 4',6-diamidino-2-phenylindole; PI, Propidium Iodide; qRT-PCR, Reverse Transcription Quantitative PCR; GO, the Gene Ontology; KEGG, the Kyoto Encyclopedia of Genes and Genomes; IGF2, Insulin-like Growth Factor 2; IGF1, Insulin-like Growth Factor 1; JUN, Jun Proto-Oncogene; MAPK3, Mitogen-activated protein kinase 3; SLK, Ste20-Like Kinase; SP1, Specificity Protein 1; RAF1, RAF Proto-Oncogene Serine; ETS2, ETS Proto-Oncogene 2; EGFR, Epidermal Growth Factor Receptor; MEK1, Mitogen-activated protein kinase kinase 1; PCA, Principal Component Analysis; DEGs, differentially expressed genes; KITLG, Kit ligand; CACNA2D1, delta subunit 1; CHUK, Conserved helix-loop-helix ubiquitous kinase; MAP2K7, Mitogen-activated protein kinase kinase 7; RB1, Retinoblastoma 1; LIFR, Leukemia inhibitory factor receptor; RND3, Rho family GTPase 3; ARHGAP5, Rho GTPase-activating protein 5; MUC1, Mucin 1; MET, Mesenchymal-epithelial transition factor; G6PD, Glucose-6-phosphate dehydrogenase; ATRX, Alpha-thalassemia; TCGA, The Cancer Genome Atlas; RhoA, Ras homolog family member A; CDK6, Cyclin-dependent kinase 6; BRAT1, BRCA1-associated protein 1; BRCA1, Breast Cancer 1; ATM, Ataxia telangiectasia mutated; ATR, Ataxia Telangiectasia and Rad3-related protein; CHK1, Checkpoint kinase 1; PIK3R2, Phosphoinositide-3-kinase regulatory subunit 2; PI3K-AKT, Phosphoinositide 3-kinase-Protein kinase B; CASP3, Caspase-3; CDH1, Cadherin-1; AKT1, v-akt murine thymoma viral oncogene homolog 1; PIK3CB, Phosphatidylinositol-4,5-bisphosphate3-kinase catalytic subunit beta.

Address correspondence to: Fang Li and Xiongwei Fan, College of Life Sciences, Hunan Normal University, Changsha 410081, Hunan, China. Tel: +86-13667365934; E-mail: li-evans@hotmail.com (FL); Tel: +86-15074863860; E-mail: fan_xiongwei@163.com (XWF); Lilu Guo, Hunan Provincial Key Laboratory of Regional Hereditary Birth Defects Prevention and Control, Changsha Hospital for Maternal and Child Health Care Affiliated to Hunan Normal University, Changsha 410007, Hunan, China. Tel: +86-13755163527; E-mail: guoll-001@163.com

References

[1] Abu-Rustum NR, Yashar CM, Arend R, Barber E, Bradley K, Brooks R, Campos SM, Chino J, Chon HS, Crispens MA, Damast S, Fisher CM, Frederick P, Gaffney DK, Gaillard S, Giuntoli R, Glaser S, Holmes J, Howitt BE, Lea J, Mantia-Smaldone G, Mariani A, Mutch D, Nagel C, Nekhlyudov L, Podoll M, Rodabaugh K, Salani R, Schorge J, Siedel J, Sisodia R, Soliman P, Ueda S, Urban R, Wyse E, McMillian NR, Aggarwal S and Espinosa S. NCCN guidelines® insights: cervical cancer, version 1.2024. J Natl Compr Canc Netw 2023; 21: 1224-1233.

[2] Cohen PA, Jhingran A, Oaknin A and Denny L. Cervical cancer. Lancet 2019; 393: 169-182.

[3] Shrestha AD, Neupane D, Vedsted P and Kallestrup P. Cervical cancer prevalence, incidence and mortality in low and middle income countries: a systematic review. Asian Pac J Cancer Prev 2018; 19: 319-324.

[4] Johnson CA, James D, Marzan A and Armaos M. Cervical cancer: an overview of pathophysiology and management. Semin Oncol Nurs 2019; 35: 166-174.

[5] Di Fiore R, Suleiman S, Drago-Ferrante R, Subbannayya Y, Pentimalli F, Giordano A and Calleja-Agius J. Cancer stem cells and their possible implications in cervical cancer: a short review. Int J Mol Sci 2022; 23: 5167.

[6] Yang SL, Tan HX, Niu TT, Liu YK, Gu CJ, Li DJ, Li MQ and Wang HY. The IFN-γ-IDO1-kynureine pathway-induced autophagy in cervical cancer cell promotes phagocytosis of macrophage. Int J Biol Sci 2021; 17: 339-352.

[7] Zeng Q, Lv C, Qi L, Wang Y, Hao S, Li G, Sun H, Du L, Li J, Wang C, Zhang Y, Wang X, Ma R, Wang T and Li Q. Sodium selenite inhibits cervical cancer progression via ROS-mediated suppression of glucose metabolic reprogramming. Life Sci 2024; 357: 123109.

[8] Mahmood HA, Tomas Bort E, Walker AJ, Grose RP and Chioni AM. FGF signalling facilitates cervical cancer progression. FEBS J 2022; 289: 3440-3456.

[9] Lee MY and Shen MR. Epithelial-mesenchymal transition in cervical carcinoma. Am J Transl Res 2012; 4: 1-13.

[10] Balasubramaniam SD, Balakrishnan V, Oon CE and Kaur G. Key molecular events in cervical cancer development. Medicina (Kaunas) 2019; 55: 384.

[11] Volkova LV, Pashov AI and Omelchuk NN. Cervical carcinoma: oncobiology and biomarkers. Int J Mol Sci 2021; 22: 12571.

[12] Huang H, Han Q, Zheng H, Liu M, Shi S, Zhang T, Yang X, Li Z, Xu Q, Guo H, Lu F and Wang J.

MAP4K4 mediates the SOX6-induced autophagy and reduces the chemosensitivity of cervical cancer. Cell Death Dis 2021; 13: 13.
[13] Li S, Ma YM, Zheng PS and Zhang P. GDF15 promotes the proliferation of cervical cancer cells by phosphorylating AKT1 and Erk1/2 through the receptor ErbB2. J Exp Clin Cancer Res 2018; 37: 80.
[14] Li Q, Li Z, Luo T and Shi H. Targeting the PI3K/AKT/mTOR and RAF/MEK/ERK pathways for cancer therapy. Mol Biomed 2022; 3: 47.
[15] Bahar ME, Kim HJ and Kim DR. Targeting the RAS/RAF/MAPK pathway for cancer therapy: from mechanism to clinical studies. Signal Transduct Target Ther 2023; 8: 455.
[16] Kim EK and Choi EJ. Pathological roles of MAPK signaling pathways in human diseases. Biochim Biophys Acta 2010; 1802: 396-405.
[17] Ullah R, Yin Q, Snell AH and Wan L. RAF-MEK-ERK pathway in cancer evolution and treatment. Semin Cancer Biol 2022; 85: 123-154.
[18] Lewis TS, Shapiro PS and Ahn NG. Signal transduction through MAP kinase cascades. Adv Cancer Res 1998; 74: 49-139.
[19] Seger R and Krebs EG. The MAPK signaling cascade. FASEB J 1995; 9: 726-735.
[20] Rasi Bonab F, Baghbanzadeh A, Ghaseminia M, Bolandi N, Mokhtarzadeh A, Amini M, Dadashzadeh K, Hajiasgharzadeh K, Baradaran B and Bannazadeh Baghi H. Molecular pathways in the development of HPV-induced cervical cancer. EXCLI J 2021; 20: 320-337.
[21] Pashirzad M, Khorasanian R, Fard MM, Arjmand MH, Langari H, Khazaei M, Soleimanpour S, Rezayi M, Ferns GA, Hassanian SM and Avan A. The therapeutic potential of MAPK/ERK inhibitors in the treatment of colorectal cancer. Curr Cancer Drug Targets 2021; 21: 932-943.
[22] Braicu C, Buse M, Busuioc C, Drula R, Gulei D, Raduly L, Rusu A, Irimie A, Atanasov AG, Slaby O, Ionescu C and Berindan-Neagoe I. A comprehensive review on MAPK: a promising therapeutic target in cancer. Cancers (Basel) 2019; 11: 1618.
[23] Xu W, Wang Y, Zhou J, Zhu X, Zhang S, Yuan W, Liu X, Shi Y, Cao L, Zeng Q, Jiang Z, Ye X, Wan Y, Peng X, Deng Y, Chen F, Wang X, Dai G, Luo S, Fan X, Mo X, Wu X and Li Y. Cardiac specific overexpression of hHole attenuates isoproterenol-induced hypertrophic remodeling through inhibition of extracellular signal-regulated kinases (ERKs) signalling. Curr Mol Med 2016; 16: 515-523.
[24] Yang B, Cai Y, Zhu P, Jiang Z, Ao J, Zhang Q, Yuan W, Peng Z, Chen J, Wen Y, Chen Y, Wang Y, Shi Y, Zhu X, Ye X, Li F, Zhuang J, Wu X, Li Y and Fan X. Transmembrane protein 121 as a novel inhibitor of cervical cancer metastasis. Exp Ther Med 2022; 24: 572.
[25] Zhou J, Li Y, Liang P, Yuan W, Ye X, Zhu C, Cheng Y, Wang Y, Li G, Wu X and Liu M. A novel six-transmembrane protein hhole functions as a suppressor in MAPK signaling pathways. Biochem Biophys Res Commun 2005; 333: 344-352.
[26] Vidal M, Gigoux V and Garbay C. SH2 and SH3 domains as targets for anti-proliferative agents. Crit Rev Oncol Hematol 2001; 40: 175-186.
[27] Ram T, Singh AK, Kumar A, Singh H, Pathak P, Grishina M, Khalilullah H, Jaremko M, Emwas AH, Verma A and Kumar P. MEK inhibitors in cancer treatment: structural insights, regulation, recent advances and future perspectives. RSC Med Chem 2023; 14: 1837-1857.
[28] Yang Z, Liu S, Wang Y, Chen Y, Zhang P, Liu Y, Zhang H, Zhang P, Tao Z and Xiong K. High expression of KITLG is a new hallmark activating the MAPK pathway in type A and AB thymoma. Thorac Cancer 2020; 11: 1944-1954.
[29] Zhang Y, Li L, Liang P, Zhai X, Li Y and Zhou Y. Differential expression of microRNAs in medulloblastoma and the potential functional consequences. Turk Neurosurg 2018; 28: 179-185.
[30] Petrosino M, Novak L, Pasquo A, Turina P, Capriotti E, Minicozzi V, Consalvi V and Chiaraluce R. The complex impact of cancer-related missense mutations on the stability and on the biophysical and biochemical properties of MAPK1 and MAPK3 somatic variants. Hum Genomics 2023; 17: 95.
[31] Lacorazza HD. Pharmacological inhibition of the MAP2K7 kinase in human disease. Front Oncol 2024; 14: 1486756.
[32] Göktuna SI. IKBKE-driven TPL2 and MEK1 phosphorylations sustain constitutive ERK1/2 activation in tumor cells. EXCLI J 2022; 21: 436-453.
[33] Knudsen ES, Pruitt SC, Hershberger PA, Witkiewicz AK and Goodrich DW. Cell cycle and beyond: exploiting new RB1 controlled mechanisms for cancer therapy. Trends Cancer 2019; 5: 308-324.
[34] Bian SB, Yang Y, Liang WQ, Zhang KC, Chen L and Zhang ZT. Leukemia inhibitory factor promotes gastric cancer cell proliferation, migration, and invasion via the LIFR-Hippo-YAP pathway. Ann N Y Acad Sci 2021; 1484: 74-89.
[35] Jie W, Andrade KC, Lin X, Yang X, Yue X and Chang J. Pathophysiological functions of Rnd3/RhoE. Compr Physiol 2015; 6: 169-186.
[36] Su L, Agati JM and Parsons SJ. p190RhoGAP is cell cycle regulated and affects cytokinesis. J Cell Biol 2003; 163: 571-582.
[37] Zhang AM, Chi XH, Bo ZQ, Huang XF and Zhang J. MUC1 gene silencing inhibits proliferation, invasion, and migration while promoting apop-

tosis of oral squamous cell carcinoma cells. Biosci Rep 2019; 39: BSR20182193.
[38] Kumar P, Ji J, Thirkill TL and Douglas GC. MUC1 is expressed by human skin fibroblasts and plays a role in cell adhesion and migration. Biores Open Access 2014; 3: 45-52.
[39] Hamouda AEI, Schalla C, Sechi A, Zenke M, Schneider RK and Hieronymus T. Met-signaling controls dendritic cell migration in skin by regulating podosome formation and function. J Invest Dermatol 2023; 143: 1548-1558. e1513.
[40] Zhang Q, Ni Y, Wang S, Agbana YL, Han Q, Liu W, Bai H, Yi Z, Yi X, Zhu Y, Sai B, Yang L, Shi Q, Kuang Y, Yang Z and Zhu Y. G6PD upregulates Cyclin E1 and MMP9 to promote clear cell renal cell carcinoma progression. Int J Med Sci 2022; 19: 47-64.
[41] Lu F, Fang D, Li S, Zhong Z, Jiang X, Qi Q, Liu Y, Zhang W, Xu X, Liu Y, Zhu W and Jiang L. Thioredoxin 1 supports colorectal cancer cell survival and promotes migration and invasion under glucose deprivation through interaction with G6PD. Int J Biol Sci 2022; 18: 5539-5553.
[42] Aguilera P and López-Contreras AJ. ATRX, a guardian of chromatin. Trends Genet 2023; 39: 505-519.
[43] Klein RM, Spofford LS, Abel EV, Ortiz A and Aplin AE. B-RAF regulation of Rnd3 participates in actin cytoskeletal and focal adhesion organization. Mol Biol Cell 2008; 19: 498-508.
[44] Sahai E, Olson MF and Marshall CJ. Cross-talk between Ras and Rho signalling pathways in transformation favours proliferation and increased motility. EMBO J 2001; 20: 755-766.
[45] Zandvakili I, Lin Y, Morris JC and Zheng Y. Rho GTPases: Anti- or pro-neoplastic targets? Oncogene 2017; 36: 3213-3222.
[46] Héraud C, Pinault M, Lagrée V and Moreau V. p190RhoGAPs, the ARHGAP35- and ARHGAP5-encoded proteins, in health and disease. Cells 2019; 8: 351.
[47] Dai L, Chen X, Zhang H, Zeng H, Yin Z, Ye Z and Wei Y. RND3 transcriptionally regulated by FOXM1 inhibits the migration and inflammation of synovial fibroblasts in rheumatoid arthritis through the Rho/ROCK pathway. J Interferon Cytokine Res 2022; 42: 279-289.
[48] Basbous S, Paysan L, Sena S, Allain N, Hiriart JB, Dugot-Senant N, Rousseau B, Chevret E, Lagrée V and Moreau V. Silencing of RND3/RHOE inhibits the growth of human hepatocellular carcinoma and is associated with reversible senescence. Cancer Gene Ther 2022; 29: 437-444.
[49] Sugiura R, Satoh R and Takasaki T. ERK: a double-edged sword in cancer. ERK-dependent apoptosis as a potential therapeutic strategy for cancer. Cells 2021; 10: 2509.
[50] Goel S, Bergholz JS and Zhao JJ. Targeting CDK4 and CDK6 in cancer. Nat Rev Cancer 2022; 22: 356-372.
[51] O'Leary B, Finn RS and Turner NC. Treating cancer with selective CDK4/6 inhibitors. Nat Rev Clin Oncol 2016; 13: 417-430.
[52] Gao X, Leone GW and Wang H. Cyclin D-CDK4/6 functions in cancer. Adv Cancer Res 2020; 148: 147-169.
[53] Fassl A, Geng Y and Sicinski P. CDK4 and CDK6 kinases: from basic science to cancer therapy. Science 2022; 375: eabc1495.
[54] So EY and Ouchi T. The potential role of BRCA1-associated ATM activator-1 (BRAT1) in regulation of mTOR. J Cancer Biol Res 2013; 1: 1001.
[55] Popova NV and Jücker M. The role of mTOR signaling as a therapeutic target in cancer. Int J Mol Sci 2021; 22: 1743.
[56] Lal MA, Bae D, Camilli TC, Patierno SR and Ceryak S. AKT1 mediates bypass of the G1/S checkpoint after genotoxic stress in normal human cells. Cell Cycle 2009; 8: 1589-1602.
[57] Duggal S, Jailkhani N, Midha MK, Agrawal N, Rao KVS and Kumar A. Defining the Akt1 interactome and its role in regulating the cell cycle. Sci Rep 2018; 8: 1303.
[58] Hinz N and Jücker M. Distinct functions of AKT isoforms in breast cancer: a comprehensive review. Cell Commun Signal 2019; 17: 154.
[59] Virard F, Giraud S, Bonnet M, Magadoux L, Martin L, Pham TH, Skafi N, Deneuve S, Frem R, Villoutreix BO, Sleiman NH, Reboulet J, Merabet S, Chaptal V, Chaveroux C, Hussein N, Aznar N, Fenouil T, Treilleux I, Saintigny P, Ansieau S, Manié S, Lebecque S, Renno T and Coste I. Targeting ERK-MYD88 interaction leads to ERK dysregulation and immunogenic cancer cell death. Nat Commun 2024; 15: 7037.